Diffusion of Knots along DNA Confined in Nanochannels

Zixue Ma and Kevin D. Dorfman*

Department of Chemical Engineering and Materials Science, University of Minnesota – Twin Cities, 421 Washington Ave SE, Minneapolis, Minnesota 55455, USA

E-mail: dorfman@umn.edu

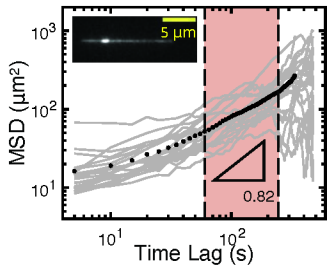

Abstract

We study the diffusion of knots along relaxed DNA in nanochannels using a nanofluidic "knot factory" device for knot generation. The apparent scaling exponent for the growth in the ensemble-averaged mean-squared displacement is 0.82 ± 0.01 when accounting for random errors, and [0.79, 0.88] when accounting for systematic errors. Both estimates indicate subdiffusion and support a model of self-reptation. These results contradict the prevailing theory for knot diffusion along nanochannel-confined DNA, where knot region breathing is presumed to control knot diffusion in long polymers, but are consistent with previous observations of self-reptation of knots for unconfined DNA under tension.

1 Introduction

Knots are intriguing topological objects, ubiquitous *in vivo* for polymeric materials such as DNA and proteins,[1–3] and the subject of considerable work in the context of polymer physics.[4] In particular, knot diffusion was first studied by simulations in linear DNA under tension[5] and nanochannel confinement.[6] Our study addresses the mechanism of knot diffusion, which remains an open question. Two diffusion mechanisms for knots in polymers have been proposed. The first is self-reptation,[7,8] where the diffusion of a knot originates from a snakelike motion of the polymer chain. Meltzer *et al.*,[9] however, proposed an additional knot diffusion mechanism: knot region breathing. This second mechanism posits that the diffusive motion of a knot is due to knot size fluctuations, locally exchanging DNA chain inside the knot region with its neighborhood. In their analysis of knot diffusion, Meltzer *et al.*[9] predicted the time-scales of a knot moving along a polymer chain for these two mechanisms. The knot diffusion time for the self-reptation mechanism scales as L^3, where L is the contour length of the polymer. In contrast, knot region breathing gives an L^2 scaling. As a consequence, this scaling argument predicts that, for long chains, the diffusion time for knot region breathing dominates self-reptation. Simulations, which provide a more detailed model of the knot diffusion, indicated that the diffusion mechanism of knots is a mix of the two mechanisms,[10] and are thus inconclusive.

While measuring knot diffusion as a function of polymer molecular weight is one possible way to distinguish between the two diffusion mechanisms, this is a challenging approach because a wide range of molecular weights are needed. A less technically difficult option is to examine the nature of the diffusion process. Knot region breathing is suggested to show normal diffusion.[9] Self-reptation, however, is thought to be subdiffusive in long polymers owing to an analogy between the reptation of the polymer through the knotted region and the translocation of a polymer through a narrow pore.[9] In the latter case, simulations[11,12] of a long polymer translocating through a narrow pore exhibit subdiffusive behavior with an exponent of 0.92 arising from the aggregate motion of the long polymer constraining the

translocation process.[12]

Ultimately, it is desirable to resolve the question of the dynamical properties of knots in unconfined polymers experimentally, but this is challenging because the polymers in free solutions undergo a random walk in three dimensions, giving rise to a difficulty detecting knots and tracking knot motion along single polymers. This challenge has been tackled by using optical tweezers[13] or by entraining the polymers in an extensional flow where polymers are trapped at the stagnation point to keep the knot within the focal plane and linearize the polymer.[14–18] Bao *et al.*[13] have examined the motion of knots along DNA linearized by optical tweezers and indicated that the knot diffusion mechanism is self-reptation. The self-reptation mechanism also agrees with the study of knot motion in DNA stretched by an extensional flow field.[17] The subdiffusive behavior of the knot, however, may be confounded by the external force used to linearize polymers. Thus, it is desirable to perform similar measurements on relaxed DNA.

Nanochannel confinement provides an approach to linearize DNA by compression instead of tension,[19] leading to relaxed DNA ends. While confinement affects the friction opposing DNA motion,[20] the increased resistance to motion would only affect the time-scale for knot diffusion and not the underlying mechanism. It is possible that confinement could also affect the knots, but this is unlikely due to the tightness of the knots.[8,21–24] Our experiments take advantage of the "knot factory" device developed by Amin *et al.*,[25] composed of nanochannel arrays with slit barriers in the center of the nanochannels. This device produces knots when a pressure-driven flow compresses a single DNA molecule against the slit barrier, where the applied pressure and waiting time can be adjusted to control the knotting probability.

Here we use T4 DNA confined in nanochannels to determine whether knot diffusion is dominated by self-reptation or knot region breathing. There are two reasons for using this molecule. First, T4 DNA, which has higher molecular weight compared with λ-DNA, was chosen to provide a high knotting probability.[26,27] Second, in the theory of Meltzer *et al.*,[9] the knot diffusion time for self-reptation is predicted to be an order of magnitude larger

than that of the knot region breathing mechanism for this molecular weight.[9] Such a large difference in predicted knot diffusion times permits an unambiguous test of the knot diffusion mechanism by inspection of the exponent governing the growth of the ensemble-averaged mean-squared displacement of the knots on time lag, where normal diffusion indicates a knot region breathing mode and subdiffusion indicates a self-reptation mode.

2 Experimental Methods

2.1 Device fabrication

The nanofluidic device shown in Figure 1a, consisting of 89 nanochannels (450 μm long) with 1 μm breaks in the channel centers and adjoining nanoslits, was designed based on the knot factory concept.[25] The arm length and the width of the two U-shaped microchannels are 8 mm and 50 μm, respectively. The devices were fabricated on fused silica substrates (University Wafers) using two steps of electron beam lithography to create first the nanochannels and then the slit barriers, and subsequent photolithography to fabricate two parallel U-shaped microchannels connecting the ends of the nanochannel array to inlet and outlet reservoirs. The connecting slits were wider than the nanochannels to simplify the alignment process during the second step of electron beam lithography. Each patterning step was followed by a fluorine (CF_4:CHF_3) reactive ion etching (RIE) step to transfer the pattern into the substrate. Scanning electron microscopy (SEM) imaging of the nanofluidic device (Figure 1b) reveals that the nanochannels are 304 nm wide and nanoslits are 500 nm wide. The depths of microchannels, nanochannels and nanoslits were measured to be 0.8 μm, 340 nm and 32 nm, respectively, using a KLA Tensor P-7 profilometer. After a standard RCA clean, the device with sand-blasted holes for sample loading was sealed with a 170 μm thick fused silica coverslip (University Wafers) via fusion bonding.

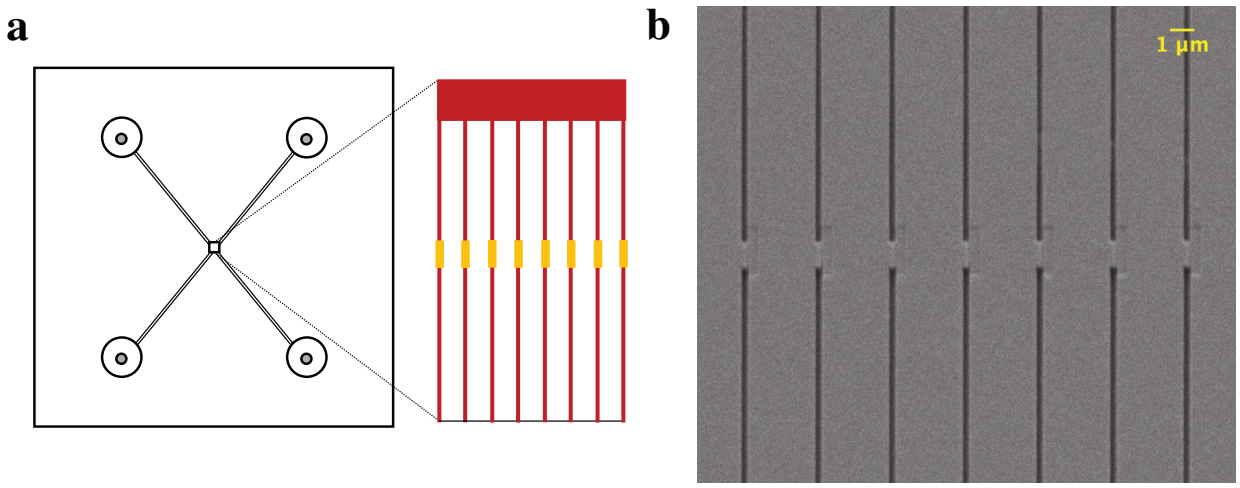

Figure 1: Knot factory device design.[25] (a) Schematic layout of the nanofluidic device with a magnified view of the nanochannels and nanoslits (not to scale). (b) SEM image of the nanochannel pattern in the nanofluidic device for knot generation. Nanochannels (black lines) are connected by slit barriers.

2.2 DNA preparation

The T4 GT7 DNA molecules (166 kilobase pairs, Nippon Gene) were stained with YOYO-1 fluorescent dye (Invitrogen) at a dye to DNA base pair ratio of 1:10 in a 5× TBE buffer solution and subsequently diluted to 0.25× TBE. The contour length, L, of the stained T4 GT7 DNA was estimated to be 65 µm by assuming an increase in the rise of 0.51 nm per intercalated YOYO-1 molecule.[28,29] The stained solution was heated at 50 °C for three hours to accelerate the equilibration of YOYO-1 binding to DNA molecules and melt any annealed DNA sticky ends.[30–32] β-mercaptoethanol (Sigma-Aldrich, 4% v/v) was added to the solution before the start of the knot diffusion experiments to suppress photobleaching of YOYO-1. The ionic strength of the final DNA sample solution is 18 mM, calculated following a previous approach.[33,34]

2.3 Knot diffusion experiments

At the start of the experiment, one microchannel of the nanofluidic device shown in Figure 1a was filled by capillary action with a buffer solution containing β-mercaptoethanol (Sigma-

Aldrich, 4% v/v) with the same ionic strength as the DNA sample solution. The DNA sample solution was then loaded to the other microchannel using a pipette. The wet device was assembled into a chuck that allows pressure actuation.[33,35] T4 DNA molecules in the microchannel were drawn into the nanochannels by applying 35 kPa pressure for around 10 s and then reducing the pressure to 10 kPa until the DNA reach the slit barriers. The DNA were then imaged prior to compression using a blue laser (Coherent OBIS, 473 nm) with a power of 2.5 mW and a 100× (1.4 N.A.) oil immersion objective on an inverted epifluorescene microscope (Olympus IX73). The images of the DNA were recorded by an EMCCD camera (Photometrics, Cascade II:512) at 20 fps with a 50 ms exposure time for 60 s to measure the DNA extension prior to compression. The T4 DNA were then compressed against the nanoslits by applying 5 kPa pressure for 60 s. Subsequently, the DNA were moved away from the nanoslit by imposing 10 kPa pressure in the opposite direction and then relaxed in the absence of any imposed pressure for 120 s before imaging. To obtain data for knot diffusion, the DNA with knots were imaged at 5 fps with a 200 ms exposure time for 8 minutes in a quiescent fluid. After video acquisition, the DNA were driven out of the nanochannels by applying 10 kPa pressure for 120 s and new DNA were loaded into the nanochannels.

After each experiment, which consists of multiple loading and compression cycles, the device was cleaned and dried to be reused for the next experiment. First, the device was immersed in DI water overnight to reduce the ionic strength of the solution in the channels. Then, the device was submerged in base piranha solution heated at 80 °C for 40 minutes to remove organic residues. The cleaned device was subsequently heated at 1000 °C for 6 hours for drying.

2.4 Data processing

The videos were processed using a custom-written MATLAB script[36] that outputs the time evolution of each DNA molecule's intensity profile. The location of left end, x_{end}, and the total extension, X, of the DNA molecule are identified by fitting the intensity profile to a dual

error-function algorithm, which is the result of a Gaussian point-spread function convolved with a box function.[37] The longest relaxtion time is computed by fitting the extension autocorrelation function with an exponential function, following a previous method.[33] The longest relaxation times of unknotted DNA and knotted DNA are 2.7 ± 0.3 s and 4.6 ± 0.4 s, respectively. The average extension of the DNA is then determined from uncorrelated measurements of its extension by using a time sampling of 5 s for unknotted DNA and 10 s for knotted DNA.

When a molecule with a knot is produced from the first image processing program, the knot position, x_{knot}, is located by using a second custom-written MATLAB program following the method described in Ref. 38. The dimensionless knot position, x_{KNOT}, is defined as

$$x_{\mathrm{KNOT}}(t) = \frac{x_{\mathrm{knot}}(t) - \langle x_{\mathrm{end}}(t) \rangle_{1\mathrm{s}}}{\langle \mathrm{X}(t) \rangle_{1\mathrm{s}}} \tag{1}$$

where $\langle \ldots \rangle_{1\mathrm{s}}$ operation is a moving average with a window length of one second to reduce the impact of chain end fluctuations.

The time evolution of independent measurements of the dimensionless knot position with a time sampling of 5 s, x_{KNOT}, is used to compute the ensemble-averaged mean-squared displacement (MSD)

$$\mathrm{MSD}(\delta t) = L^2 \left\langle [x_{\mathrm{KNOT}}(t) - x_{\mathrm{KNOT}}(t - \delta t)]^2 \right\rangle_{\mathrm{t,n}} \tag{2}$$

where $\langle \ldots \rangle_{\mathrm{t,n}}$ is an average over time t and the ensemble of n DNA molecules and δt is the time lag between images.[39] When useful, we will also refer to a time-averaged MSD, which corresponds to applying Eq. 2 to a single knot's trajectory without averaging over n.

To analyze the diffusive behavior of the ensemble of knots, we computed the scaling exponent β of the ensemble-averaged data for the MSD by fitting the logarithm of the data with a linear function

$$\log_{10} \mathrm{MSD}(\delta t) = \beta \log_{10} \delta t + c \tag{3}$$

where both β and c are fitted constants. At short time lags, the dynamic diffusion coefficient, MSD/$2\delta t$, decays continuously until the time lag of 60 s, as shown in Figure 2a, due to a dynamic error in the MSD.[40] Thus, the lower bound for the time lag used for the calculation of the exponent β is determined to be 60 s. The choice of upper bounds requires a quantitative approach. We first calculate the correlation coefficient, R^2, of the linear fit line with different upper bounds and a fixed lower bound of 60 s. We then performed two analyses, by considering the random error and the systematic error caused by the choice of the upper bound separately. The upper bound determined from the first analysis is 255 s, which is the point with the highest R^2 value. For the second analysis, the upper bounds larger than 150 s are selected where R^2 value is greater than 0.99. Thus, the upper bound has a range [150 s, 325 s] for estimation of systematic errors. The minimum upper bound is determined to be 150 s because the time-averaged MSDs of the various knots fluctuate significantly when time lags are greater than 150 s, as shown in Figure 2b. This fluctuation is mainly caused by limited statistics.[39] As a result, two choices of the upper bound are 255 s for estimating the random error and [150 s, 325 s] for estimating the systematic error.

3 Results

Our device was designed based on the nanofluidic knot factory device developed by Amin *et al.*[25] to generate knots with high probability. The effective size of our nanochannels, corresponding to the geometric mean of channel sizes after correcting for the DNA-wall excluded volume and electrostatic interactions, is 308 nm.[39,41,42] This effective size is close to the knot factory device effective channel size of 346 nm from Amin *et al.*,[25] which we computed from their reported channel sizes and the ionic strength of their buffer solution. With this effective channel size, the knotting probability of our device is expected to be close to prior work[25] because the knotting probability is presumed to be a function of channel size.[43–45] For the applied pressure and waiting time used in our experiments, we anticipated

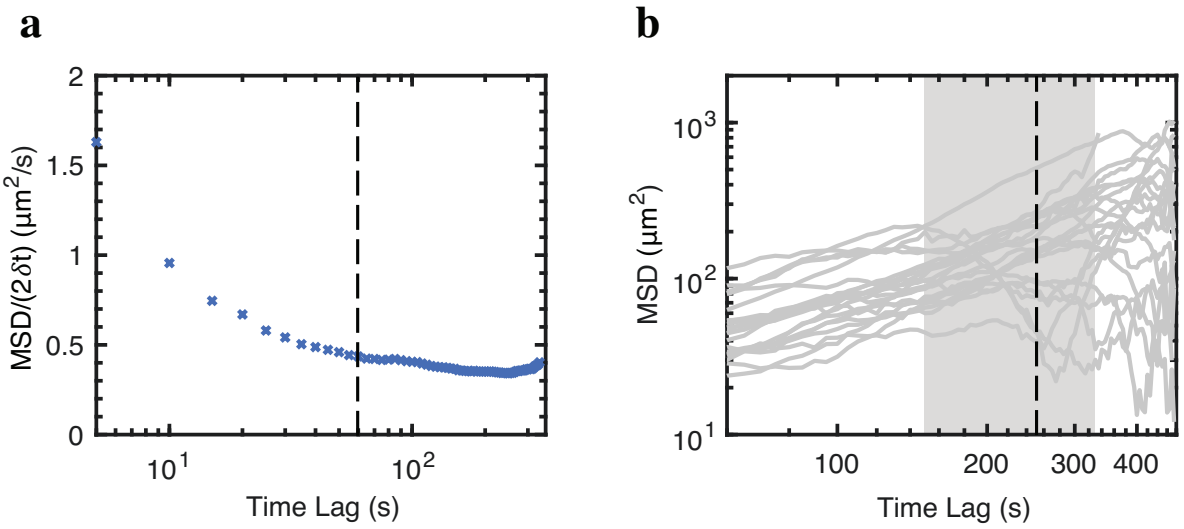

Figure 2: Determination of lower and upper bounds of the time lag used for fitting the scaling exponent β. (a) Dynamic diffusion coefficient, MSD/$2\delta t$, as a function of time lag. The MSD/$2\delta t$ decays continuously to a constant value of around 0.4 $\mu m^2/s$ at the time lag of 60 s, indicated by the vertical black dashed line. (b) Time-averaged MSDs as a function of time lag for individual knots. The figure shows the large fluctuations of the time-averaged MSDs for individual knots at time lags larger than 150 s. The vertical black dashed line indicates the first choice of the upper bound of 255 s for estimating the random error. The shaded region corresponds to the second choice of the range of upper bounds from 150 s to 325 s for estimating the systematic error.

a knotting probability of around 60 % based on the model for the probability of forming a single knot from Amin *et al.*[25] The probability of knot generation in our experiments on 42 molecules was 48 ± 20 % calculated using a Clopper-Pearson interval with a 95 % confidence interval.[46] Our knotting probability is consistent with the prediction from previous work.[25]

The T4 DNA molecules with an estimated contour length of 65 μm[28,29] are susceptible to shear cleavage by hydrodynamic forces during the compression required to generate knots.[47] We thus performed two control analyses, one measuring the effect of the compression step and the other checking the quality of the DNA initially loaded into the device, to confirm that shear cleavage was sufficiently small that it would not affect the knot diffusion mechanism, which is expected to be a function of the polymer chain length.[9]

The first test we performed was to analyze the change in DNA length after compression against the slit barrier. Since only half of our molecules are knotted, we can examine

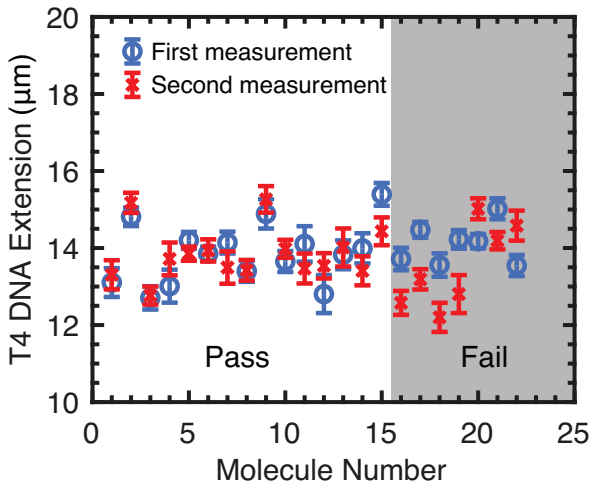

Figure 3: Average extension for unknotted T4 DNA molecules from uncorrelated measurements of their extension before and after compressed against nanoslits. The error bars are the standard error of the mean. The shaded region represents the 7 rejected molecules, which are 1.1 ± 0.1 μm shorter after being compressed against the nanoslits.

whether T4 DNA molecules are sheared significantly by compression against the nanoslits by examining those DNA molecules that do not form knots during the compression. To this end, Figure 3 compares the average extension for 22 unknotted T4 DNA molecules before and after being compressed against the nanoslits. An unpaired two-sample t test with 5 % significance level was used to determine if the two-measurement means are equal. The test result shows that 15 molecules passed the hypothesis test. The rejected 7 molecules are 1.1 ± 0.1 μm shorter after compressed against the nanoslits. This is a relatively small effect on the DNA size.

In addition to the average extension of unknotted DNA before and after compression, we also measured the chain extension distribution of the T4 DNA molecules before knots are formed in those DNA. The extension of long DNA molecules is linear in chain length.[48] Figure 4 provides the distribution of T4 DNA extension in nanochannels from uncorrelated measurements of their extension, showing that the T4 DNA extension values are spread around the mean value 14.6 μm with a standard error of 0.2 μm. Our effective channel size of 308 nm is in the extended de Gennes regime, which corresponds to effective channel sizes

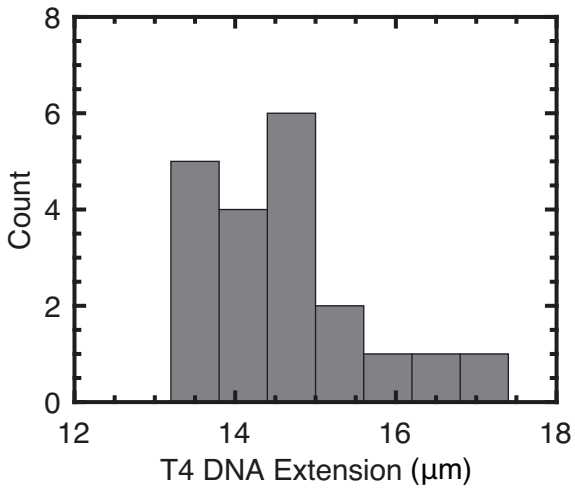

Figure 4: Histogram of the extension distribution of the T4 DNA before knot generation. The mean value of the extensions is 14.6 μm with a standard error of 0.2 μm, corresponding to a fractional extension of 0.22 based on a contour length of 65 μm.

ranging from 241 nm to 694 nm estimated based on simulations.[49] Theory for confined polymers in the extended de Gennes regime predicts a fractional extension of 0.23 for our channel size.[50] The corresponding average contour length of these observed T4 DNA molecules is estimated to be 63.5 ± 0.9 μm based on the measured average extension and the theory-based prediction of fractional extension, remarkably close to the expected value for intact, stained T4 DNA.[50] While the theory of knot diffusion mechanisms suggests a strong scaling of knot diffusion time with polymer chain length,[9] this narrow range of observed T4 DNA chain length in Figure 4 and the small amount of shear cleavage during compression observed in Figure 3 lead us to conclude that variations in molecular weight between different molecules are not expected to affect the mechanism of knot diffusion.

Figure 5a shows an example of knot diffusion along a DNA chain confined in a nanochannel; the knot is visualized as a bright spot that moves along the less bright background of the unknotted portion of the DNA chain with time, and the white streak is the knot trajectory. Such a bright feature could also be associated with a fold.[38,51] A folded configuration, however, unfolds spontaneously via an entropic force.[52] The typical unfolding time is about 30 s for a fold with an initial length of about 8 μm.[51] Such folds were also observed in our

experiments after the compression process, but they were unfolded before the knot diffusion measurements. Knots, on the other hand, are persistent, localized and only unravel at the chain end.[13,17,25] Thus, the argument that the bright feature is a knot in our device is strongly supported by the differences between knots and folds in their unravelling processes. Figure 5b illustrates a time trace of position of the knot produced by processing the kymograph shown in Figure 5a.

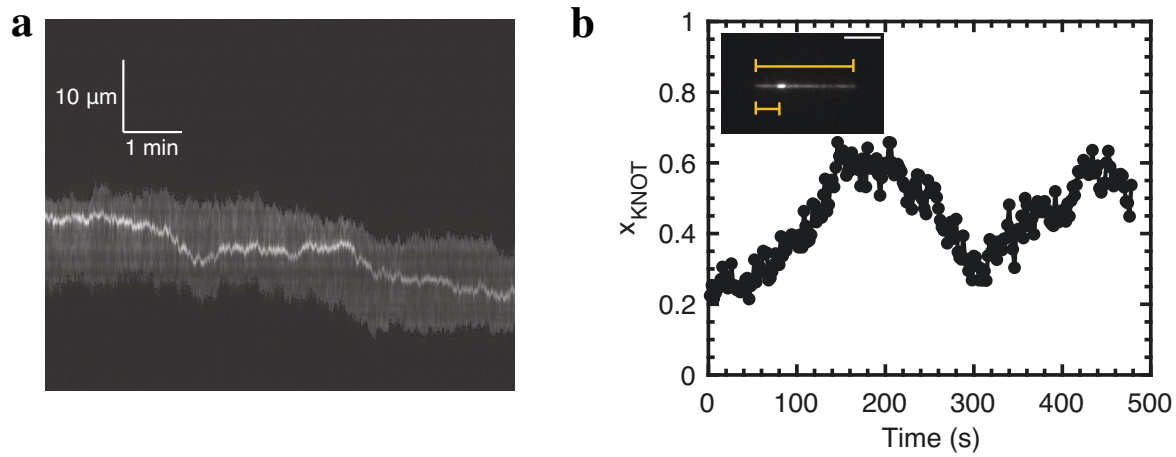

Figure 5: Trajectory of a knot along the DNA molecule. (a) Kymograph of a T4 DNA after a knot is formed in our device. The vertical axis is intensity along the nanochannel and the horizontal axis is time. The knot is observed as a bright spot that diffuses along the less bright background of the unknotted portion of DNA chain. Black boxes at the ends of the DNA images are created by the imaging processing code to locate the DNA molecule. (b) Time trace of the knot in (a) diffusing along the DNA chain confined in a nanochannel. The dimensionless knot position, x_{KNOT}, is defined as the ratio of the knot's distance from DNA left end to the DNA extension in Eq. 1, as illustrated in the inset of a knotted DNA molecule image. The scale bar is 5 μm.

The evolution of the dimensionless single knot positions in time allows us to compute the time-averaged mean-squared displacement (MSD) of each knot. Figure 6 shows the time-averaged MSDs for individual knots along with the ensemble-averaged MSD as a function of time lag; time-averaged MSDs reveal greater statistical uncertainty than the ensemble-averaged MSD. Thus, knot diffusive behavior is quantified by using the ensemble-averaged MSD to improve the estimation of the scaling exponent characterizing the knot diffusive behavior.[53] The apparent scaling exponent extracted by fitting the ensemble-averaged MSD

data between 60 s and 255 s in Figure 6 is 0.82 ± 0.01, where the error refers to a 95% confidence interval from the linear regression. For upper bounds from 150 s to 325 s, the range of the scaling exponent is [0.79, 0.88], where the range indicates the systematic error due to the choice of the upper bound for the linear regression. Both results indicate a subdiffusive behavior of knots along T4 DNA chains confined in nanochannels.

Two potential sources of systematic error are that each knot generated in the knot factory device may have (i) a different topology[54,55] and (ii) a different initial position relative to the chain ends. While we expect the scaling exponent, which characterizes the knot diffusive behavior, is insensitive to the type of knot,[13,56] checking the topological complexity of analyzed knots could further verify the accuracy of the scaling exponent of the ensemble-averaged MSD. We cannot directly ascertain the knot complexity from the images, but we can create a proxy for the knot complexity by comparing the knot dynamic diffusion constants in Figure 7 because the dynamic diffusion constant is suggested to decrease with complexity of knots, consistent with slower diffusion for larger knots.[13] The dynamic diffusion constant is calculated as $\mathrm{MSD}/2\delta t$ at a fixed time lag of 60 s to avoid tracking noise and limited statistics.[17,57] The scatter plot illustrates no apparent correlation between knot dynamic diffusion constant and knot fraction for the ensemble of observed knots, suggesting that the knots we observe are of similar (but unknown) complexity. The position of a knot relative to the chain ends, however, is expected to affect the scaling exponent of knot diffusion. The knot mobility is thought to increase when a knot moves towards one of the chain ends.[9,17] Figure 8 shows that there is no apparent relationship between the MSD at a time lag of 60 s and the initial knot position relative to the chain ends for the ensemble measured knots. The experimental result of our observed knots is inconclusive for the effect of initial knot positions on knot diffusion due to insufficient data.

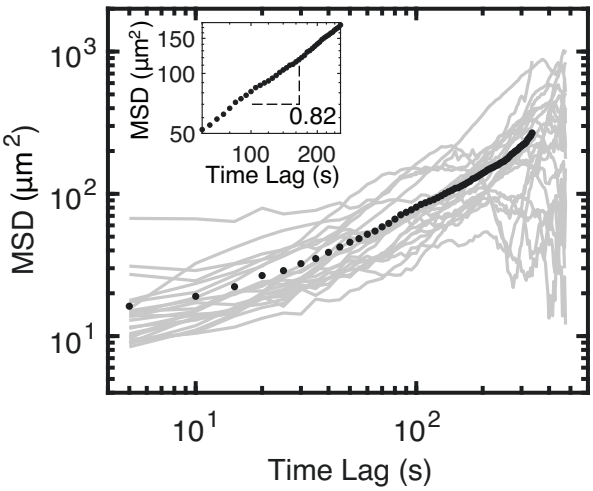

Figure 6: Mean-squared displacements as a function of time lag. The gray solid lines, which also appear in Figure 2b, are time-averaged MSDs for individual knots. The black dots are the ensemble-averaged MSD of the ensemble of knots as a function of time lag. The linear fit to the logarithm of ensemble-averaged MSD and time lag data between 60 s and 255 s yields a scaling exponent of 0.82 ± 0.01, as illustrated in the inset. The error is estimated using a 95% confidence interval. The determinations of lower and upper bounds of the time lag used in the inset for fitting were described in Figure 2.

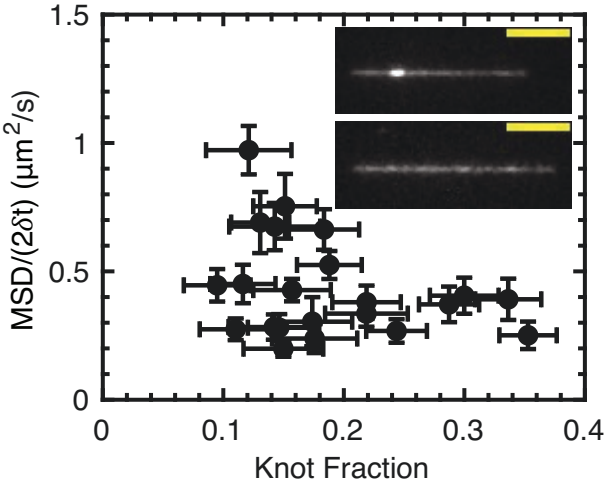

Figure 7: Scatter plot of the knot dynamic diffusion constants, defined as MSD/$2\delta t$, at a time lag of 60 s and knot fractions for an ensemble of measured knots. The knot fraction is defined as a ratio of extension difference between unknotted and knotted DNA chain to the unknotted DNA chain extension. The inset shows the images of nanochannel confined knotted T4 DNA (top) and the DNA before knot generation (bottom). The scale bars are 5 μm.

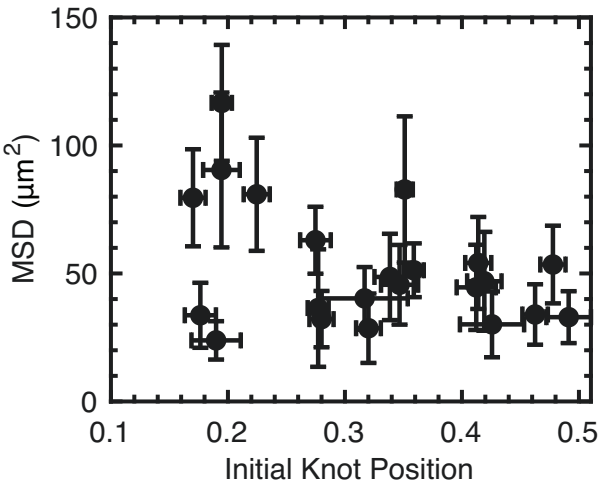

Figure 8: Scatter plot of the time-averaged MSDs at a time lag of 60 s and initial positions relative to the chain ends for the observed knots. The initial dimensionless knot position is defined as the ratio of the knot's distance from either of the chain ends to the DNA extension at 0 s.

4 Discussion

Our observations of knot movement along T4 DNA chains reveal that the motion of knots is subdiffusive with an apparent scaling exponent of 0.82 ± 0.01 at the range of time lags between 60 s and 255 s, where the uncertainty is an estimate of the random error, and a scaling exponent range [0.79, 0.88] produced by the possible systematic errors from the choice of the upper bound for the exponent. Those values are not the same as the predicted value of 0.92 from simulations of long self-avoiding polymers translocating through a narrow pore.[11] The translocation process is analogous to the knot self-reptation mechanism,[11,12] but it is difficult to rigorously compare the two scaling exponents due to the differences between the two systems. In our experiment, DNA knots translate along extended chains under nanochannel confinement. The pore translocation, however, is a process that polymers move through a narrow pore in a membrane with infinite space on both sides of the membrane.

The subdiffusive behavior of knots observed in our experiments contradicts the theory proposed by Meltzer *et al.*[9] for the diffusion of DNA knots in nanochannels. At the contour length of T4 DNA, the rate of knot region breathing prediction by Meltzer *et al.*[9] is

about an order of magnitude faster than self-reptation, implying that knot region breathing should dominate knot diffusion along T4 DNA. Based on their theory, the knot movement along T4 DNA should be regular diffusion, inconsistent with our results of knot subdiffusive behavior. The inconsistency is plausibly due to the assumption of Brownian diffusion by Meltzer *et al.*[9] for both diffusion mechanisms when predicting the scaling of knot diffusion time with polymer chain length, a point which is noted in their analysis. Another factor accounting for this discrepancy might be the narrow range of the measured knot diffusion due to experimental limitations. Surmounting these limitations is non-trivial, requiring very even longer DNA molecules (e.g., yeast choromosomes), very high stability of the stage, and the use of stroboscopic imaging to provide adequate coverage over the full range of time lags. The knot diffusive behavior at later time lags larger than the upper bound $\delta t = 325$ s from our experiments is thus inconclusive due to the lack of sufficient data at such long time lags.

Our observation of subdiffusion of knots agrees with the results from experimental[17] and theoretical[58] studies of dynamics of knots along polymers under tension. Klotz *et al.*[17] found anomalous behavior of knots in T4 DNA stretched by an elongational field in a microfluidic device. The MSD of the knot position measured in their experiments[17] shows subdiffusive behavior at short time lags and superdiffusion at long time lags. The superdiffusive behavior agrees with a prediction from an asymmetric self-reptation mechanism, where knots are expected to move faster towards one of the chain ends.[9,17] Their observation[17] of knot subdiffusive behavior in T4 DNA at short time lags less than around 50 s is consistent with our experimental results. Our experimental results are also supported by simulations by Matthews *et al.*,[58] who found subdiffusive motion of knots along strected polymer chains at short times.

The observed subdiffusive behavior of knots, however, is not consistent with the simulation results of Matthews *et al.*[58] at larger times and computational studies on knot diffusion along stretched DNA chain under tension,[5] which show normal diffusive behavior. This discrepancy may be due to the difference between stretched chains under tension and

nanochannel confined chains in the extended de Gennes regime. In stretched chains, the knot moves along the polymer contour, which is aligned along the observed axis. A confined polymer in the extended de Gennes regime, however, corresponds to a series of anisometric blobs with a tortuous chain.[50] Our experiments measure the knot diffusion projected onto the channel axis, which is not necessarily the same as the knot diffusion along the chain contour. A study of more extended DNA chains in Odijk regime is a potential method to reduce the difference of measured knot diffusion track between stretched and confined chains, since the chain tortuosity would be largely eliminated.[59]

Our experimental results also suggest directions in modeling DNA knot diffusion for further theoretical studies. One issue is the low effective ionic strength of the buffer solution of 18 mM in our experiment, lower than the salt condition of 100 mM assumed in previous simulations.[5,6,58] The effect of electrostatics might need to be incorporated into simulation models for DNA knot diffusion, which typically treat the polymer as neutral with an increased persistence length (and, where applicable, effective width) due to electrostatic repulsion. However, the more important consideration is that the analysis of simulation data likely does not discriminate between small and large knots. Indeed, the identification of small knots is relatively straightforward in simulations but challenging for experiments.[5,6,56,58,60–62] The knots generated in our experiment are estimated to contain several microns of contour length. Simulations with complex and large knots are needed to make a thorough comparison to our experimental data. At the same time, if computational studies of small knots indicate a measurable difference in diffusive behavior between small and large knots, they could motivate developing experimental methods to visualize those small knots.

5 Conclusion

We have examined the diffusion of knots along DNA molecules confined in nanochannels by using a nanofluidic device to generate knots and fluorescence microscopy to observe knot

movement. The knot diffusive behavior was quantified by a scaling exponent of ensemble-averaged mean-squared displacement on time lag. The apparent scaling exponent and the range of scaling exponents were found to be 0.82 ± 0.01, where the uncertainty refers to the random error, and [0.79, 0.88], where the range indicates the systematic error, both indicating a subdiffusive behavior of knots along DNA molecules. Our finding contradicts the theory[9] that knot diffusion is dominated by knot region breathing, but agrees with observations of the short-time dynamics of knots on DNA under tension.[17,58] Our experimental work also provides guidelines to model knot diffusion along DNA for future simulation studies.

While the observation of knot subdiffusive behavior supports the self-reptation mechanism, it is desirable in the future to measure diffusion time of knots along DNA molecules with different contour length to test definitively the two knot diffusion models; it may be the case that the crossover between knot region breathing and self-reptation takes place at a higher molecular weight than predicted by Meltzer *et al.*[9] Other open questions related to knot dynamics still remain, particularly the details surrounding the effect of confinement, which is controlled by channel size and the ionic strength of buffer solution, on knot diffusion. The effect of knots on DNA chain diffusion in different confinement regimes[49,63] is also a particularly intriguing question.

Acknowledgement

We thank Dr. Hui-Min Chuang for assistance in device fabrication protocols. This work was supported by NIH (R01-HG006851) and NSF (CBET-2016879). Device fabrication was conducted in the Minnesota Nano Center, which is supported by the National Science Foundation through the National Nano Coordinated Infrastructure Network (NNCI) under Award Number ECCS-1542202.

References

(1) Meluzzi, D.; Smith, D. E.; Arya, G. Biophysics of knotting. *Annu. Rev. Biophys.* **2010**, *39*, 349–366.

(2) Liu, L. F.; Perkocha, L.; Calendar, R.; Wang, J. C. Knotted DNA from bacteriophage capsids. *Proc. Natl. Acad. Sci. USA* **1981**, *78*, 5498–5502.

(3) Taylor, W. R.; Lin, K. Protein knots: a tangled problem. *Nature* **2003**, *421*, 25–25.

(4) Orlandini, E. Statics and dynamics of DNA knotting. *J. Phys. A: Math. Theor.* **2018**, *51*, 053001.

(5) Vologodskii, A. Brownian dynamics simulation of knot diffusion along a stretched DNA molecule. *Biophys. J.* **2006**, *90*, 1594–1597.

(6) Micheletti, C.; Orlandini, E. Knotting and unknotting dynamics of DNA strands in nanochannels. *ACS Macro Lett.* **2014**, *3*, 876–880.

(7) Dommersnes, P. G.; Kantor, Y.; Kardar, M. Knots in charged polymers. *Phys. Rev. E* **2002**, *66*, 031802.

(8) Grosberg, A. Y.; Rabin, Y. Metastable tight knots in a wormlike polymer. *Phys. Rev. Lett.* **2007**, *99*, 217801.

(9) Metzler, R.; Reisner, W.; Riehn, R.; Austin, R.; Tegenfeldt, J. O.; Sokolov, I. M. Diffusion mechanisms of localised knots along a polymer. *EPL (Europhysics Letters)* **2006**, *76*, 696–702.

(10) Möbius, W.; Frey, E.; Gerland, U. Spontaneous unknotting of a polymer confined in a nanochannel. *Nano Lett.* **2008**, *8*, 4518–4522.

(11) Chuang, J.; Kantor, Y.; Kardar, M. Anomalous dynamics of translocation. *Phys. Rev. E* **2001**, *65*, 011802.

(12) Kantor, Y.; Kardar, M. Anomalous dynamics of forced translocation. *Phys. Rev. E* **2004**, *69*, 021806.

(13) Bao, X. R.; Lee, H. J.; Quake, S. R. Behavior of complex knots in single DNA molecules. *Phys. Rev. Lett.* **2003**, *91*, 265506.

(14) Soh, B. W.; Klotz, A. R.; Doyle, P. S. Untying of complex knots on stretched polymers in elongational fields. *Macromolecules* **2018**, *51*, 9562–9571.

(15) Soh, B. W.; Narsimhan, V.; Klotz, A. R.; Doyle, P. S. Knots modify the coil-stretch transition in linear DNA polymers. *Soft Matter* **2018**, *14*, 1689–1698.

(16) Narsimhan, V.; Klotz, A. R.; Doyle, P. S. Steady-state and transient behavior of knotted chains in extensional fields. *ACS Macro Lett.* **2017**, *6*, 1285–1289.

(17) Klotz, A. R.; Soh, B. W.; Doyle, P. S. Motion of knots in DNA stretched by elongational fields. *Phys. Rev. Lett.* **2018**, *120*, 188003.

(18) Klotz, A. R.; Narsimhan, V.; Soh, B. W.; Doyle, P. S. Dynamics of DNA knots during chain relaxation. *Macromolecules* **2017**, *50*, 4074–4082.

(19) Dai, L.; Doyle, P. S. Comparisons of a polymer in confinement versus applied force. *Macromolecules* **2013**, *46*, 6336–6344.

(20) Muralidhar, A.; Dorfman, K. D. Kirkwood diffusivity of long semiflexible chains in nanochannel confinement. *Macromolecules* **2015**, *48*, 2829–2839.

(21) Dai, L.; Renner, C. B.; Doyle, P. S. Origin of metastable knots in single flexible chains. *Phys. Rev. Lett.* **2015**, *114*, 037801.

(22) Dai, L.; Renner, C. B.; Doyle, P. S. Metastable tight knots in semiflexible chains. *Macromolecules* **2014**, *47*, 6135–6140.

(23) Dai, L.; Renner, C. B.; Doyle, P. S. Metastable knots in confined semiflexible chains. *Macromolecules* **2015**, *48*, 2812–2818.

(24) Katritch, V.; Olson, W. K.; Vologodskii, A.; Dubochet, J.; Stasiak, A. Tightness of random knotting. *Phys. Rev. E* **2000**, *61*, 5545.

(25) Amin, S.; Khorshid, A.; Zeng, L.; Zimny, P.; Reisner, W. A nanofluidic knot factory based on compression of single DNA in nanochannels. *Nat. Commun.* **2018**, *9*, 1506.

(26) Suma, A.; Orlandini, E.; Micheletti, C. Knotting dynamics of DNA chains of different length confined in nanochannels. *J. Phys: Condens. Matter* **2015**, *27*, 354102.

(27) Tubiana, L.; Rosa, A.; Fragiacomo, F.; Micheletti, C. Spontaneous knotting and unknotting of flexible linear polymers: Equilibrium and kinetic aspects. *Macromolecules* **2013**, *46*, 3669–3678.

(28) Kundukad, B.; Yan, J.; Doyle, P. S. Effect of YOYO-1 on the mechanical properties of DNA. *Soft Matter* **2014**, *10*, 9721–9728.

(29) Günther, K.; Mertig, M.; Seidel, R. Mechanical and structural properties of YOYO-1 complexed DNA. *Nucleic Acids Res.* **2010**, *38*, 6526–6532.

(30) Nyberg, L.; Persson, F.; Åkerman, B.; Westerlund, F. Heterogeneous staining: a tool for studies of how fluorescent dyes affect the physical properties of DNA. *Nucleic Acids Res.* **2013**, *41*, e184.

(31) Carisson, C.; Johnson, M.; Åkerman, B. Double bands in DNA gel electrophoresis caused by bis-intercalating dyes. *Nucleic Acids Res.* **1995**, *23*, 2413–2420.

(32) Lund, A. H.; Duch, M.; Skou Pedersen, F. Increased cloning efficiency by temperature-cycle ligation. *Nucleic Acids Res.* **1996**, *24*, 800–801.

(33) Gupta, D.; Sheats, J.; Muralidhar, A.; Miller, J. J.; Huang, D. E.; Mahshid, S.; Dorfman, K. D.; Reisner, W. Mixed confinement regimes during equilibrium confinement spectroscopy of DNA. *J. Chem. Phys.* **2014**, *140*, 214901.

(34) See `http://microfluidics.stanford.edu/download/CalcEquilibrium_LoC_v1p1.m` for the program for equilibrium reaction calculations.

(35) Persson, F.; Tegenfeldt, J. O. DNA in nanochannels—directly visualizing genomic information. *Chem. Soc. Rev.* **2010**, *39*, 985–999.

(36) Reisner, W.; Morton, K. J.; Riehn, R.; Wang, Y. M.; Yu, Z.; Rosen, M.; Sturm, J. C.; Chou, S. Y.; Frey, E.; Austin, R. H. Statics and dynamics of single DNA molecules confined in nanochannels. *Phys. Rev. Lett.* **2005**, *94*, 196101.

(37) Tegenfeldt, J. O.; Prinz, C.; Cao, H.; Chou, S.; Reisner, W. W.; Riehn, R.; Wang, Y. M.; Cox, E. C.; Sturm, J. C.; Silberzan, P.; Austin, R. H. The dynamics of genomic-length DNA molecules in 100-nm channels. *Proc. Natl. Acad. Sci. USA* **2004**, *101*, 10979–10983.

(38) Reifenberger, J. G.; Dorfman, K. D.; Cao, H. Topological events in single molecules of E. coli DNA confined in nanochannels. *Analyst* **2015**, *140*, 4887–4894.

(39) Gupta, D.; Bhandari, A. B.; Dorfman, K. D. Evaluation of blob theory for the diffusion of DNA in nanochannels. *Macromolecules* **2018**, *51*, 1748–1755.

(40) Savin, T.; Doyle, P. S. Static and dynamic errors in particle tracking microrheology. *Biophys. J.* **2005**, *88*, 623–638.

(41) Bhandari, A. B.; Reifenberger, J. G.; Chuang, H.-M.; Cao, H.; Dorfman, K. D. Measuring the wall depletion length of nanoconfined DNA. *J. Chem. Phys.* **2018**, *149*, 104901.

(42) Gupta, D.; Miller, J. J.; Muralidhar, A.; Mahshid, S.; Reisner, W.; Dorfman, K. D. Experimental evidence of weak excluded volume effects for nanochannel confined DNA. *ACS Macro Lett.* **2015**, *4*, 759–763.

(43) Jain, A.; Dorfman, K. D. Simulations of knotting of DNA during genome mapping. *Biomicrofluidics* **2017**, *11*, 024117.

(44) Micheletti, C.; Orlandini, E. Knotting and metric scaling properties of DNA confined in nano-channels: a Monte Carlo study. *Soft Matter* **2012**, *8*, 10959–10968.

(45) Orlandini, E.; Micheletti, C. Knotting of linear DNA in nano-slits and nano-channels: a numerical study. *J. Biol. Phys.* **2013**, *39*, 267–275.

(46) Clopper, C. J.; Pearson, E. S. The use of confidence or fiducial limits illustrated in the case of the binomial. *Biometrika* **1934**, *26*, 404–413.

(47) Davison, P. F. The effect of hydrodynamic shear on the deoxyribonucleic acid from T2 and T4 bacteriophages. *Proc. Natl. Acad. Sci. USA* **1959**, *45*, 1560–1568.

(48) Muralidhar, A.; Tree, D. R.; Wang, Y.; Dorfman, K. D. Interplay between chain stiffness and excluded volume of semiflexible polymers confined in nanochannels. *J. Chem. Phys.* **2014**, *140*, 084905.

(49) Dai, L.; van der Maarel, J.; Doyle, P. S. Extended de Gennes regime of DNA confined in a nanochannel. *Macromolecules* **2014**, *47*, 2445–2450.

(50) Werner, E.; Mehlig, B. Confined polymers in the extended de Gennes regime. *Phys. Rev. E* **2014**, *90*, 062602.

(51) Reifenberger, J. G.; Cao, H.; Dorfman, K. D. Odijk excluded volume interactions during the unfolding of DNA confined in a nanochannel. *Macromolecules* **2013**, *51*, 1172-1180.

(52) Levy, S. L.; Mannion, J. T.; Cheng, J.; Reccius, C. H.; Craighead, H. G. Entropic unfolding of DNA molecules in nanofluidic channels. *Nano Lett.* **2008**, *8*, 3839-3844.

(53) Kepten, E.; Bronshtein, I; Garini, Y. Improved estimation of anomalous diffusion exponents in single-particle tracking experiments. *Phys. Rev. E* **2013**, *87*, 052713.

(54) Rybenkov, V. V.; Cozzarelli, N. R.; Vologodskii, A. V. Probability of DNA knotting and the effective diameter of the DNA double helix. *Proc. Natl. Acad. Sci. USA* **1993**, *90*, 5307–5311.

(55) Uehara, E.; Deguchi, T. Knotting probability of self-avoiding polygons under a topological constraint. *J. Chem. Phys.* **2017**, *147*, 094901.

(56) Huang, L.; Makarov, D. E. Langevin dynamics simulations of the diffusion of molecular knots in tensioned polymer chains. *J. Phys. Chem. A* **2007**, *111*, 10338–10344.

(57) Martin, D. S.; Forstner, M. B.; Käs, J. A. Apparent subdiffusion inherent to single particle tracking. *Biophys. J.* **2002**, *83*, 2109–2117.

(58) Matthews, R.; Louis, A. A.; Yeomans, J. M. Effect of topology on dynamics of knots in polymers under tension. *EPL (Europhysics Letters)* **2010**, *89*, 20001.

(59) Odijk, T. The statistics and dynamics of confined or entangled stiff polymers. *Macromolecules* **1983**, *16*, 1340–1344.

(60) Narsimhan, V.; Renner, C. B.; Doyle, P. S. Jamming of knots along a tensioned chain. *ACS Macro Lett.* **2016**, *5*, 123–127.

(61) Dai, L.; Doyle, P. S. Universal knot spectra for confined polymers. *Macromolecules* **2018**, *51*, 6327–6333.

(62) Vandans, O.; Yang, K.; Wu, Z.; Dai, L. Identifying knot types of polymer conformations by machine learning. *Phys. Rev. E* **2020**, *101*, 022502.

(63) Odijk, T. Scaling theory of DNA confined in nanochannels and nanoslits. *Phys. Rev. E* **2008**, *77*, 060901(R).